UDC 621.3.013 https://doi.org/10.20998/2074-272X.2023.2.04

R.S. Kumar, C.S.R. Reddy, B.M. Chandra

Optimal performance assessment of intelligent controllers used in solar-powered electric vehicle

***Introduction**. Increasing vehicle numbers, coupled with their increased consumption of fossil fuels, have drawn great concern about their detrimental environmental impacts. Alternative energy sources have been the subject of extensive research and development. Due to its high energy density, zero emissions, and use of sustainable fuels, the battery is widely considered one of the most promising solutions for automobile applications. A major obstacle to its commercialization is the battery's high cost and low power density. **Purpose**. Implementing a control system is the primary objective of this work, which is employed to change the energy sources in hybrid energy storage system about the load applied to the drive. **Novelty.** To meet the control objective, a speed condition-based controller is designed by considering four separate math functions and is programmed based on different speed ranges. On the other hand, the conventional/intelligent controller is also considered to develop the switching signals related to the DC-DC converter's output and applied the actual value. **Methods.** According to the proposed control strategy, the adopted speed condition based controller is a combined conventional/intelligent controller to meet the control object. **Practical value.** In this work, three different hybrid controllers adopted speed condition based controller with artificial neural network controller, adopted speed condition based controller with fuzzy logic controller, and adopted speed condition based controller with proportional-integral derivative controller are designed and applied separately and obtain the results at different load conditions in MATLAB/Simulink environment. Three hybrid controller's execution is assessed based on time-domain specifications.* References 19, table 2, figures 40.

Key words: **solar power, proportional-integral derivative controller, artificial neural network controller, fuzzy logic controller.**

***Вступ**. Збільшення кількості транспортних засобів у поєднанні із збільшенням споживання ними викопного палива викликало серйозну заклопотаність з приводу їх згубного впливу на навколишнє середовище. Альтернативні джерела енергії були предметом інтенсивних досліджень та розробок. Завдяки високій щільності енергії, нульовим викидам та використанню екологічно чистих видів палива акумулятор широко вважається одним із найперспективніших рішень для застосувань у автомобілях. Основною перешкодою для його комерціалізації є висока вартість батареї та низька питома потужність. **Мета**. Впровадження системи управління, яка використовується для зміни джерел енергії в системі гібридної накопичення енергії в залежності від навантаження, прикладеного до приводу, є основною метою цієї роботи. **Новизна**. Для досягнення мети управління контролер на основі умов швидкості розроблено з урахуванням чотирьох окремих математичних функцій та запрограмовано на основі різних діапазонів швидкостей. З іншого боку, вважається, що звичайний/інтелектуальний контролер виробляє сигнали перемикання, пов'язані з вихідним сигналом перетворювача постійного струму, та застосовує фактичне значення. **Методи**. Відповідно до запропонованої стратегії управління прийнятий контролер на основі умов швидкості є комбінованим традиційним/інтелектуальним контролером для задоволення об'єкта управління. **Практична цінність**. У цій роботі три різних гібридних контролери, що використовують контролер на основі умов швидкості з контролером штучної нейронної мережі, контролер на основі адаптованих умов швидкості з контролером з нечіткою логікою та контролер на основі прийнятих умов швидкості з пропорційно-інтегрально-диференціальним контролером, розроблені та застосовуються окремо та отримують результати за різних умов навантаження у середовищі MATLAB/Simulink. Робота трьох гібридних контролерів оцінюється з урахуванням специфікацій у часовій області.* Бібл. 19, табл. 2, рис. 40.

Ключові слова: **сонячна енергія, пропорційно-інтегральний похідний контролер, контролер штучної нейронної мережі, контролер нечіткої логіки.**

Introduction. Most of the greenhouse content is produced from a conventional transportation system, which is harmful to the entire universe. To save the atmosphere from destructive gases released by the Internal Combustion (IC) engine-based vehicles, battery-based vehicles are introduced. Thereafter solar power-based vehicles are also designed to increase the environmentally friendly probability. Single energy source powered electric vehicles have taken some draws back like driving range and peak power production during transient state conditions. Multiple sources powered electric vehicles are again designed to drawbacks present in single-power electric vehicles. The main problem associated with multiple power source vehicles is the switching of energy sources related to the dynamics of the vehicle. In this, a different control scheme is intended to achieve the accurate transition of energy sources.

A system is designed especially for solar power-based electric vehicles. With the designed system, separate space is created for vehicles for charging the main sources [1]. The separate power system is constructed only with solar power, which is used to share the power from the conventional grid because the designed conventional power system is supplying power to general purposes like lighting, industries, and utilities. To meet the electric vehicles, load by dismissing, the burden on conventional power systems a solar power system is constructed which is exclusively for electric vehicle charging [2, 3]. A predictive controller is designed based on various nonlinearities, which are present in vehicles. Moreover, the designed controller is used for changing the energy source of solar power electric vehicles that may battery to supercapacitor vice versa [4]. The control strategy is designed with two separate controllers for an easy-shifting of energy sources of Hybrid Energy Storage System (HESS), battery, and Ultra Capacitor (UC). The designed control strategy is useful during changing energy sources precisely [5, 6]. An adaptive supervisory management control strategy is proposed for multiple energy sources powered by electric vehicles and the proposed strategy is useful to share the power between different sources present in HESS [7, 8]. Various power electronic devices are proposed to charge the battery present in plug-in electric or hybrid vehicles, in that some of the devices will take more time and some will take less time for continuous ON and OFF conditions used to control the voltage levels of converters [9, 10]. Separate fuel cell, electric and hybrid electric vehicle architectures are presented and compared to the drawbacks and advantages of those systems. Moreover, it is used to select the type of vehicle for a particular application [11].

Research focuses on the development of an echelon battery. It is possible to use echelon-use batteries in battery energy storage systems (BESS) in the power grid, but the energy management strategy should differ from that of a traditional battery [12]. The main purpose of this system is to provide sufficient energy to different loads and minimize the energy deficit and the loss of power supply probability (LPSP) [13]. For energy storage to provide multiple grid services effectively and safely, Energy Management Systems (EMSs) and optimization methods are essential [14]. With five parameters, the fractional-order controller is more flexible and robust for microgrid perturbations than the classical Proportional-Integral derivative (PID) controller. A new optimization technique called Krill Herd is used to optimize the parameters of the fractional order PID controller. Compared with other optimization methods like Particle Swarm Optimization (PSO), this is a suitable optimization method [15, 16]. For reducing the effects of PV power intermittency on the stability of the electric grid, a novel algorithm for EMS is proposed, which is combined with a storage system. EMS controls power flow from the PV generator to the grid based on the predetermined PV power level in the simulation model. The PV system and energy storage system are connected to the same DC bus [17].

Description of Photovoltaic Array (PVA). Figure 1 illustrates [18] the PVA model which is obtained from several PVA modules. The PVA includes series R_{se}, shunt R_{sh} and load R_L resistance. In the same way, the photon I_{ph}, the diode I_0, and load I_{pv} currents are represented by their flowing direction.

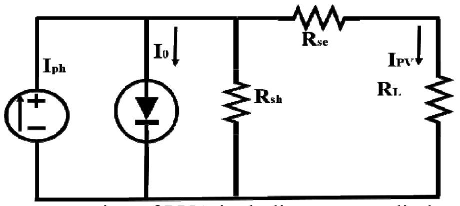

Fig. 1. Representation of PVA including source, diode, and load

The current from the input of the circuit is characterized by I_{ph}

$$I_{ph} = \left[I_{scr} + I_K \cdot (T - 298)\right] \cdot \lambda / 1000 , \qquad (1)$$

where I_K is the short-circuit current of cell at 25 °C and 1000 W/m^2; T is the junction temperature, K; λ is the solar irradiation, W/m^2.

The reverse saturation current of the module is given by

$$I_{rs} = I_{scr} / \left[\exp\left(q \cdot V_{oc} / N_S \cdot k \cdot A \cdot T\right) - 1\right]. \qquad (2)$$

Module saturation current is represented with I_0 and is given as

$$I_0 = I_{rs}\left[\frac{T}{T_r}\right]^3 \exp\left[\frac{q \cdot E_{g0}}{B \cdot k}\left\{\frac{1}{T_r} - \frac{1}{T}\right\}\right]. \qquad (3)$$

The total current of the PVA module is given as

$$I_{pv} = N_P \cdot I_0\left[\exp\left\{\frac{q \cdot \left(V_{pv} + I_{pv}R_s\right)}{N_s \cdot A \cdot k \cdot T}\right\} - 1\right], \qquad (4)$$

where I_{rs}, I_{scr}, V_{oc}, V_{pv}, I_{pv}, R_s are the reverse saturation current, short circuit current, open circuit voltage, cell voltage, cell current, and resistance of the circuit; k is the Boltzmann's constant; q is the electron charge; T_r is the nominal temperature (298.15 K); E_{g0} is the band gap energy of the semiconductor; N_s, N_p are the number of cells connected in series and in parallel, respectively; A, B are the ideality factors.

System model with proposed control configuration. The main block diagram with different sources and the solar panel is represented in Fig. 2 [5]. The major source battery is rechargeable and gets charged from the solar panel during the daytime. Here battery can discharge the energy to the load during sunlight is unavailable time. The two controller's output signal is compared at the circuit breaker block, to produce controlled switching pulses. The electric drive is connected across the DC bus, which is a combination of two DC-DC converters' outputs. The control switches shown in the block diagram are used to control the flow from the PVA to the battery and unidirectional converter (UDC). Here bidirectional converter (BDC) is used to do the two-directional operations.

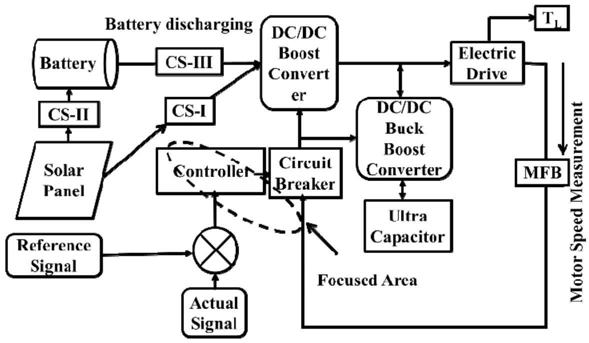

Fig. 2. Representation of the proposed scheme with a block diagram

Figure 3 [6] is representing the proposed model with DC-DC converters with three switches S_1, S_2, and S_3. Here switches S_1 and S_3 are used for boost operation whereas switch S_2 is used to perform the buck operation. The ON and OFF condition of the converts is always decided by the vehicle load condition which is again related to motor speed. The UC is associated with the BDC side, in the same way, the battery is linked at the UDC end. The main source always sends energy to load except for starting and heavy load. On the other hand, UC can send power to load during transient state conditions and gets charged from the battery during no-load periods.

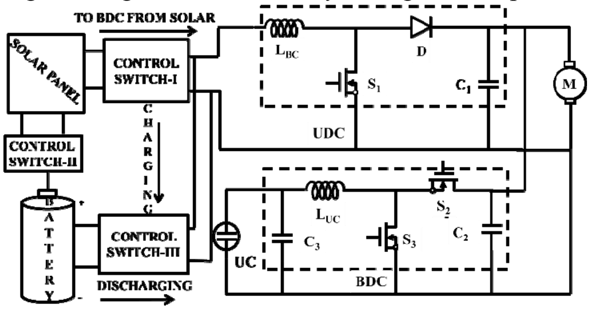

Fig. 3. Circuit representation with converters and source

About controllers used in recommended method. In this work total, four controllers were used based on the proposed control strategy. Those are Speed condition-based (SCB), Artificial Neural Network (ANN), Fuzzy Logic Controller (FLC), and PID controllers. In this section description of all controllers is given.

SCB controller is the main controller utilized in the projected control approach. This controller design is always related to the motor's speed. This will develop 4-outputs U_1, U_2, U_3, and U_4 by taking input value as speed. Depending upon the speed ranges, the particular output of SCB is in the active state, which again will decide the regulated signals to the switch existing in the BDC and UDC.

ANN controller. The general architecture of the ANN controller for obtaining the output signal is represented in Fig. 4 [19]. Here the required output of the controller always depends upon the delayed output and delayed inputs of the ANN controller. Here back propagation method is adopted to obtain the desired output from the applied converters. The z-inverse model is utilized here to send the signals from the output to the input of the network.

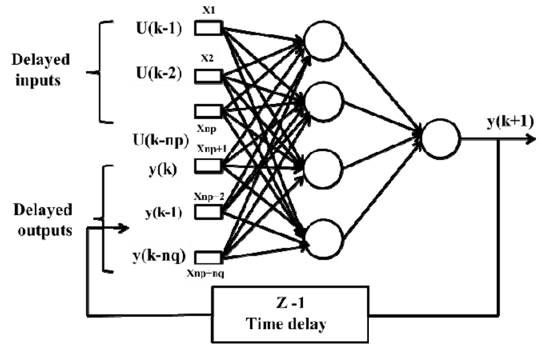

Fig. 4. The ANN controller diagrammatic representation

PID controller. The mathematical equation related to the PID controller (Fig. 5) has been represented with the below equation

$$y(t) \propto \left(e(t) + \int e(t) \mathrm{d}t + \frac{\mathrm{d}e(t)}{\mathrm{d}t} \right); \qquad (5)$$

$$y(t) = k_p \cdot e(t) + k_i \int e(t) \mathrm{d}t + k_d \frac{\mathrm{d}e(t)}{\mathrm{d}t}; \qquad (6)$$

where k_p, k_i, k_d, $e(t)$ represent the proportional, integral, derivative gains and error value.

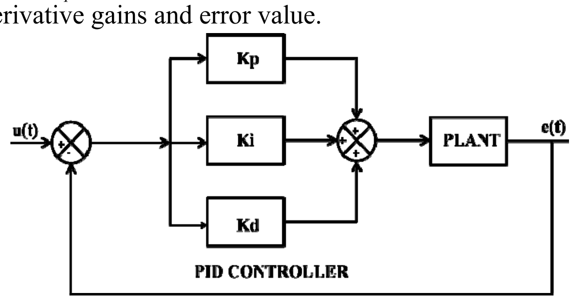

Fig. 5. PID block diagram model with three gain values

Fuzzy Logic Controller (FLC). Figure 6 [9] illustrates how FLCs are typically structured. For the output of the fuzzy logic controller to be rectified, separate mathematical modeling need not be performed. The type of membership function selected depends on the requirements of the system. Most commonly, triangular, or trapezoidal shapes are used. Afterward, the inference was performed using a rule base. Here, the output variables were managed using a rule base. The fuzzy logic controller considered each rule base to determine the result. This FLC system measures error (E) and change in error (CE) as inputs, which means FLC output is the result of error and change in error.

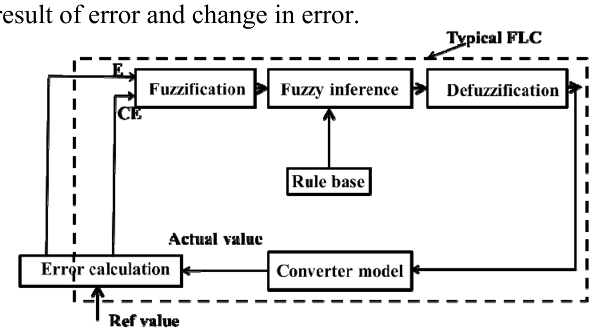

Fig. 6. General model representation of an FLC network

Main circuit with proposed technique. The main circuit operation is divided into four modes based on a load applied. In mode one, the total power demanded by the motor is supplied from the UC due to a heavy load, in mode two of operation battery, and UC combined to meet the load requirement. During mode three, the battery only supplies the load requirement, in the fourth mode of operation battery can supply power to UC as well as load. Figures 7-10 are corresponding to different modes of operation of electric motor [15].

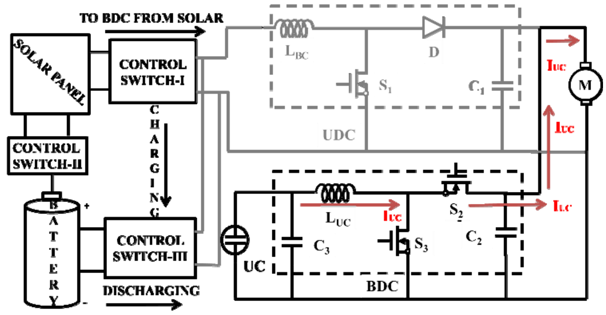

Fig. 7. Mode ONE related circuit model with BDC and UDC

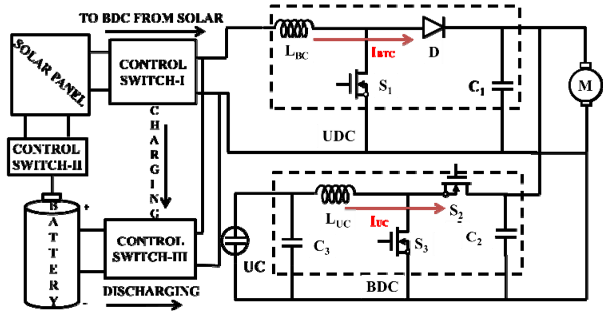

Fig. 8. Mode TWO related circuit model with BDC and UDC

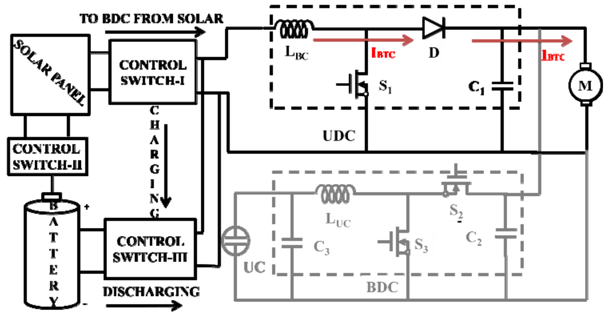

Fig. 9. Mode THREE related circuit model with BDC and UDC

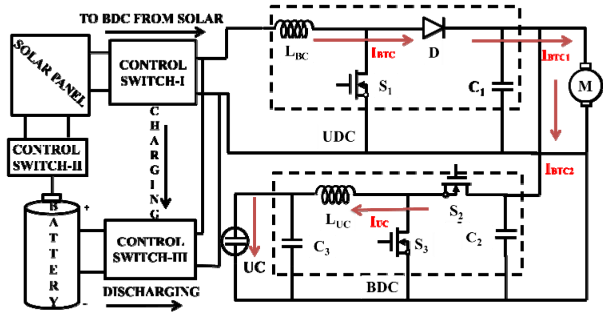

Fig. 10. Mode FOUR related circuit model with BDC and UDC

Presentation of proposed control strategy technique. Figure 11 is representing how the measured signals are generated related to the motor's speed in four modes of operation.

The SCB generates the four different output pulses as per the speed range of an electric motor as follows

1. If the $N \leq 4800$ rpm then math function U_1 only is in an active state and remaining all math functions are disabled.

2. The speed range is $4600 \leq N \leq 4800$ rpm then math functions U_1, and U_2 are in the active state and the remaining two-math function disabled state.

3. If speed is $4801 \leq N \leq 4930$ rpm then math function U_3 is in the active state and remains all are disabled.

4. The $N \geq 4931$ rpm the math function U_4 is in the active state and remain math functions are disabled.

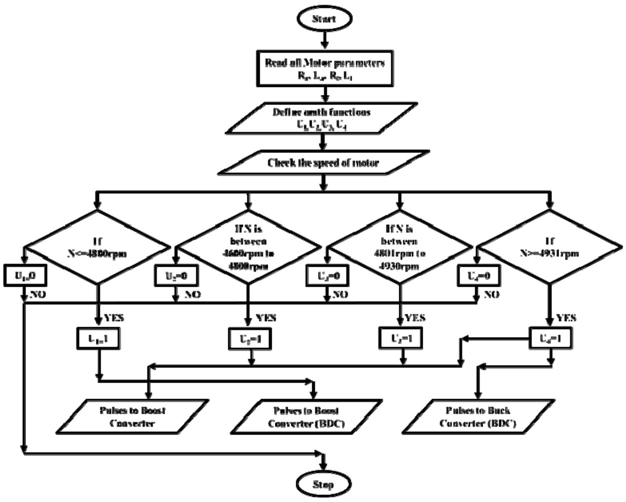

Fig. 11. Three converter pulse signal production of flow chart model

Figures 12-14 demonstrate the development of the regulated pulses to the switches S_1, S_2, and S_3 and which are obtained as per the outputs of the SCB as follows. If the output sign of the SCB is whichever U_2, or U_3, or U_4 then the regulated pulse is produced to the switch S_1. When the output of the SCB is only U_4, the regulated pulses are developed to S_2. If the output of the SCB is whichever U_1 or U_2 then the regulated pulses are offered to S_3.

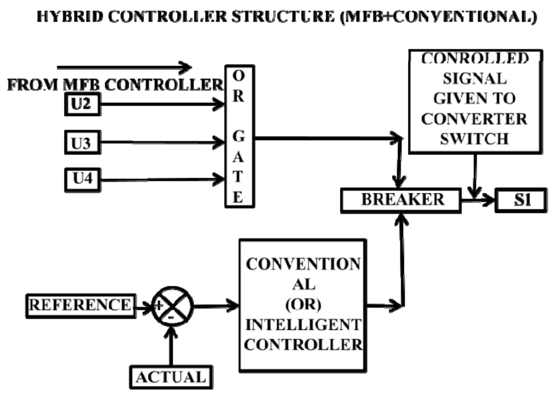

Fig. 12. Switch-1 normalized signals representation

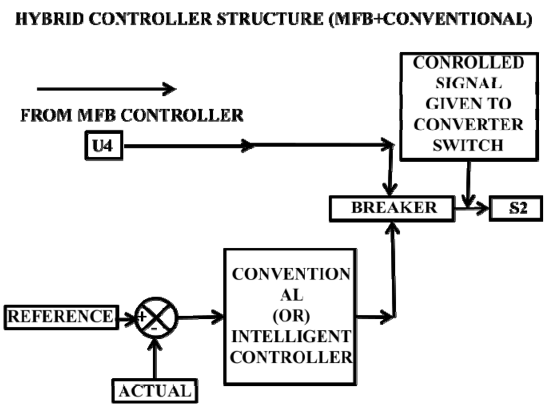

Fig. 13. Switch-2 normalized signals representation

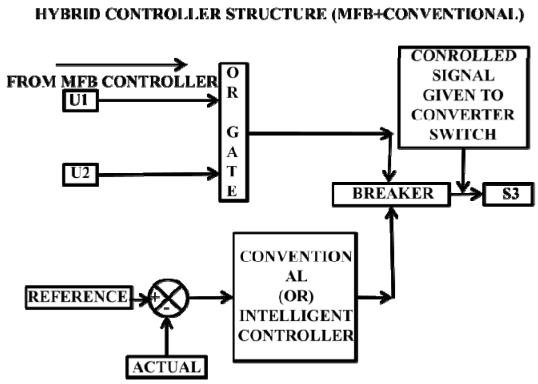

Fig. 14. Switch-3 normalized signals representation

Simulation outcomes and considerations. The outcomes after successful simulation are presented in this section. The SCB with ANN controller's speed, current, and switching signals generation plots are shown in Figures continuously 15, 21, 27, 33 and 18, 24, 30, 36. Similarly, SCB with PID output responses of a motor is represented in Figures 16, 22, 28, 34 on the other hand, Figures 19, 25, 31, 37 are indicating the switching signal delivered to a particular switch existing in BDC and UDC. Finally, SCB with fuzzy logic controller's output responses is shown in Figures 17, 23, 29 and 35 similarly. Figures 20, 26, 32, and 38 are the switching signals formed to BDC and UDC.

Mode-I results.

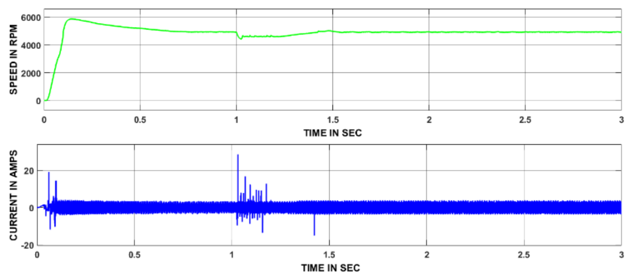

Fig. 15. Output responses of the electric drive related to Mode-I (SCB+ANN)

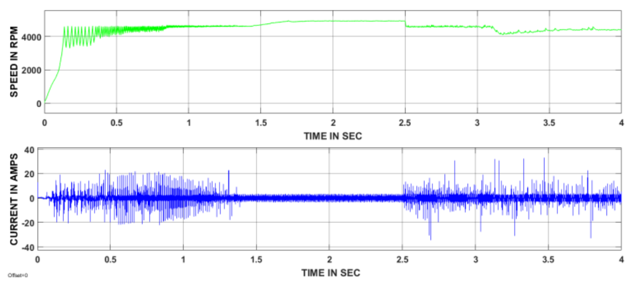

Fig. 16. Output responses of the electric drive related to Mode-I (SCB+PID)

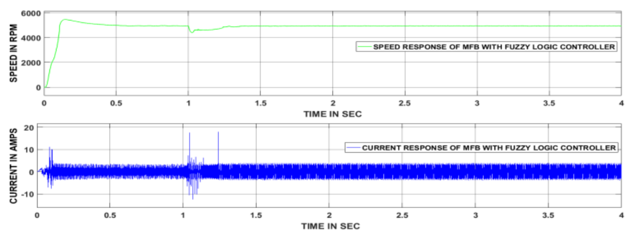

Fig. 17. Output responses of the electric drive related to Mode-I (SCB+FLC)

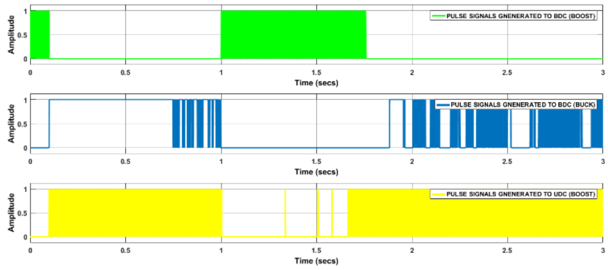

Fig. 18. Pulses of converters by SCB+ANN, Mode-I

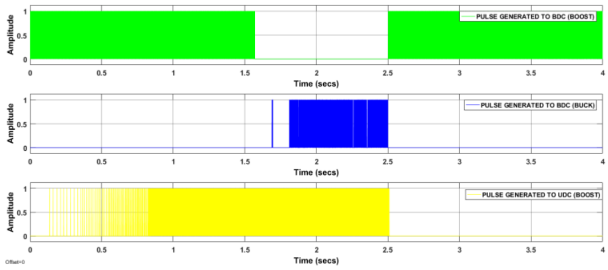

Fig. 19. Pulses of converters by SCB+PID, Mode-I

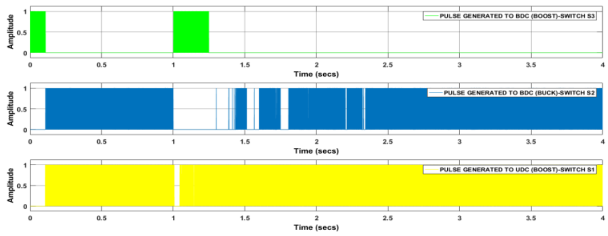

Fig. 20. Pulses of converters by SCB+FLC, Mode-I

Mode-II results.

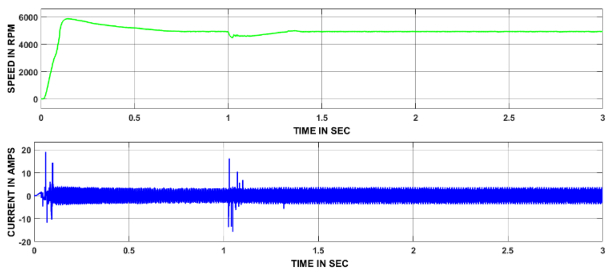

Fig. 21. Output responses of the electric drive related to Mode-II (SCB+ANN)

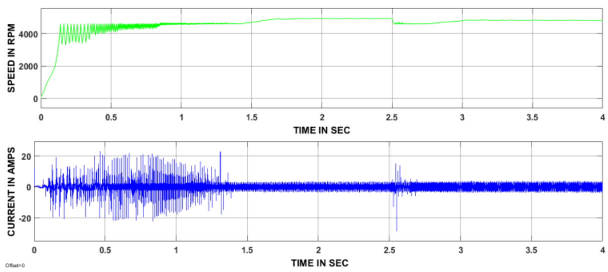

Fig. 22. Output responses of the electric drive related to Mode-II (SCB+PID)

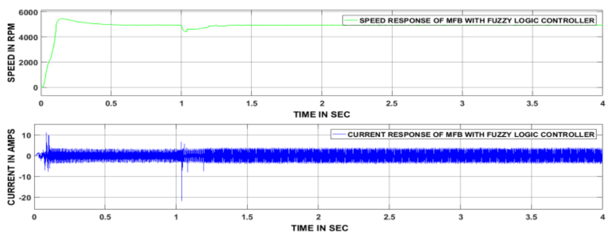

Fig. 23. Output responses of the electric drive related to Mode-II (SCB+FLC)

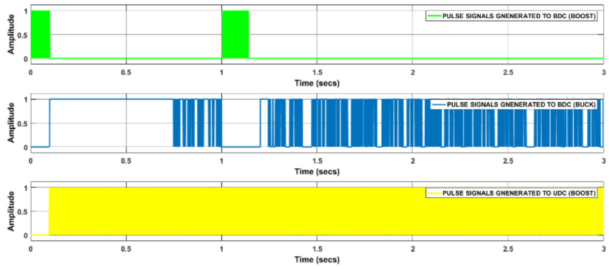

Fig. 24. Pulses of converters by SCB+ANN, Mode-II

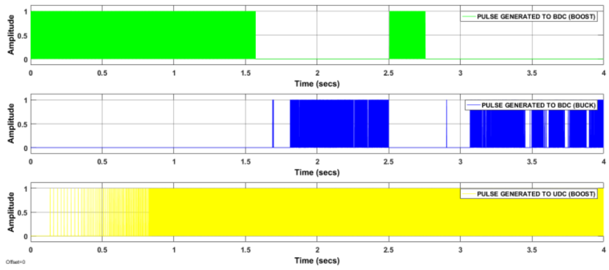

Fig. 25. Pulses of converters by SCB+PID, Mode-II

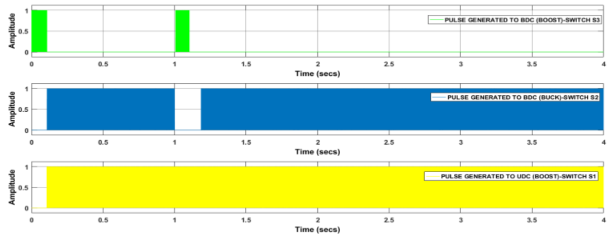

Fig. 26. Pulses of converters by SCB+FLC, Mode-II

Mode-III results.

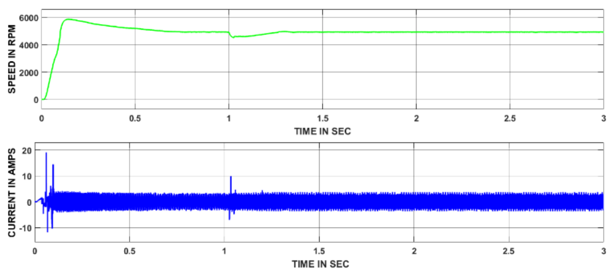

Fig. 27. Output responses of the electric drive related to Mode-III (SCB+ANN)

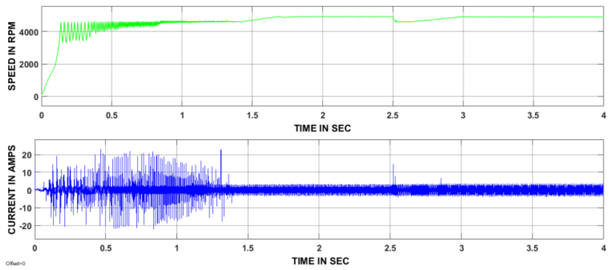

Fig. 28. Output responses of the electric drive related to Mode-I (SCB+PID)

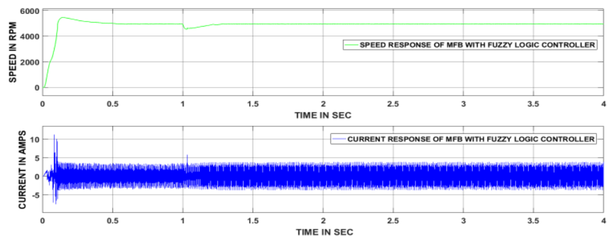

Fig. 29. Output responses of the electric drive related to Mode-I (SCB+FLC)

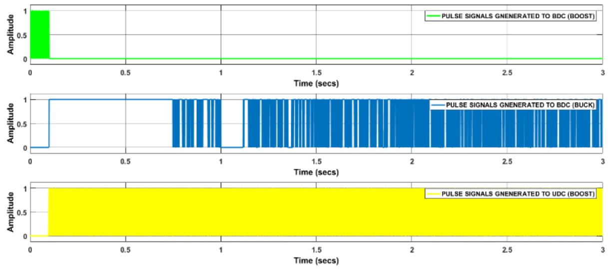

Fig. 30. Pulses of converters by SCB+ANN, Mode-III

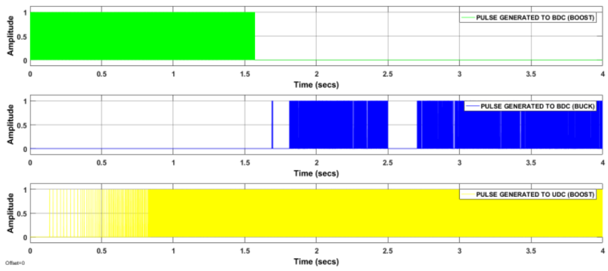

Fig. 31. Pulses of converters by SCB+PID, Mode-III

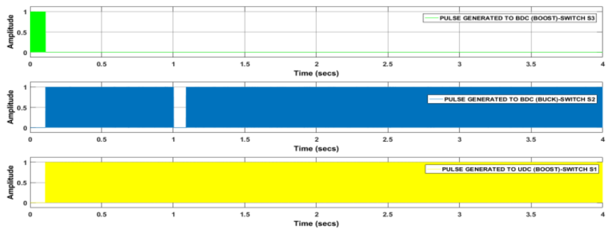

Fig. 32. Pulses of converters by SCB+FLC, Mode-III

Mode-IV results.

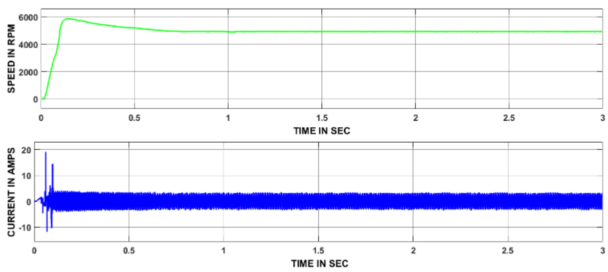

Fig. 33. Output responses of the electric drive related to Mode-IV (SCB+ANN)

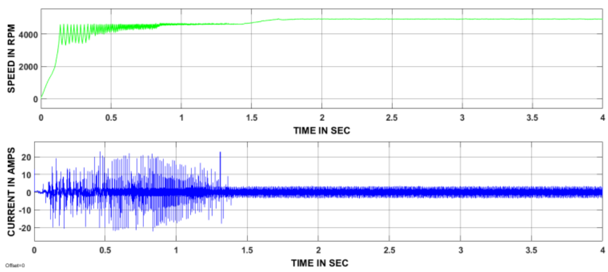

Fig. 34. Output responses of the Electric drive related to Mode-I (SCB+PID)

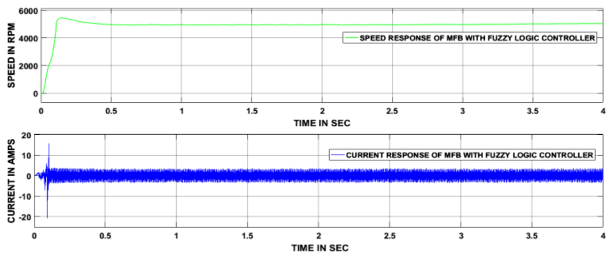

Fig. 35. Output responses of the electric drive related to Mode-I (SCB+FLC)

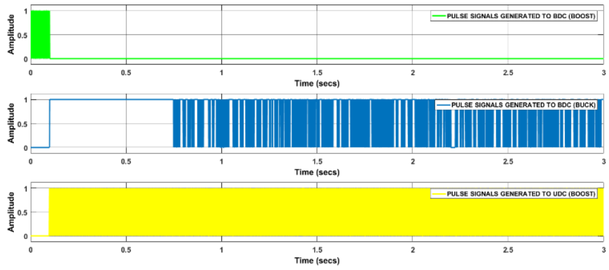

Fig. 36. Pulses of converters by SCB+ANN, Mode-IV

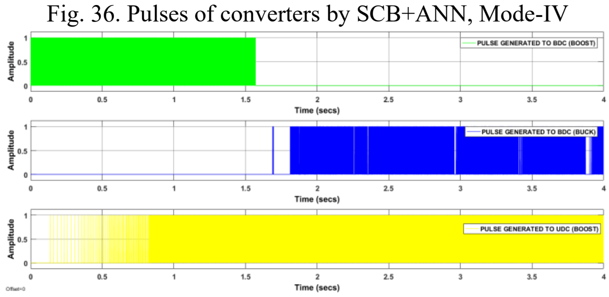

Fig. 37. Pulses of converters by SCB+PID, Mode-IV

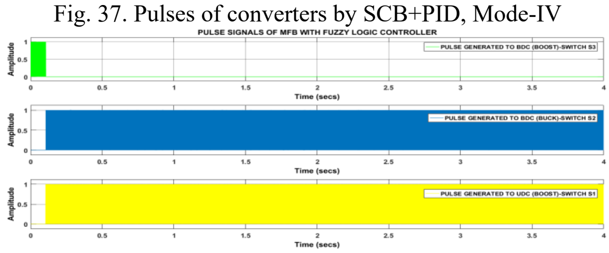

Fig. 38. Pulses of converters by SCB+FLC, Mode-IV

Battery parameters. Figure 39 represents the battery parameters which include state of charge (SOC), voltage, and current corresponding to charge and discharge. Here the positive sign of the current shows the battery charge period and a negative sign is corresponding to the discharge.

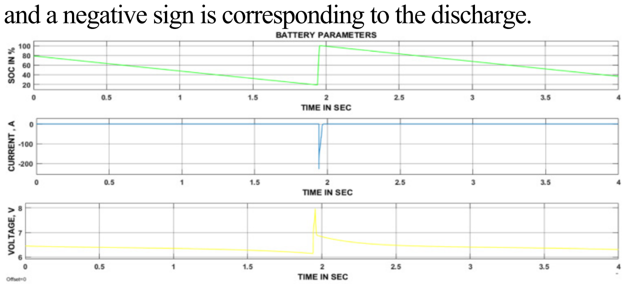

Fig. 39. Different parameters of the battery

About PVA parameters. Different inputs are provided to the solar panel to generate power at different voltage levels. Here the main input parameter of the solar panel is temperature and irradiance, based on the maximum power tracking algorithm a duty cycle is generated to the DC-DC converter of the solar panel. The provided duty cycle of the solar panel converter is always decided on the constant output voltage level corresponding to different input variations of a solar panel.

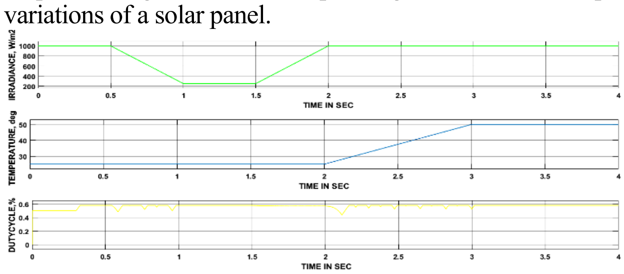

Fig. 40. Various parameters of the PVA module

Table 1 reveals the steady-state reaching for different controllers during four modes of operation. Among all the controllers SCB with ANN, FLC, and PID, responses are not reached the steady state under any load conditions.

Table 1

The controllers' performance representation based on steady-state time

Controller	Time taken by the individual controller based on the load applied, s			
	Mode-I	Mode-II	Mode-III	Mode-IV
SCB+ANN	0.75	0.25	0.10	Load free
SCB+FLC	0.25	0.15	0.11	Load free
SCB+PID	–	0.40	0.20	Load free

Table 2 shows the 3 controller's performance analyses. Among all the controllers SCB+ANN provides better results in all the aspects except maximum peak overshoot.

Table 2

Representation of three controller's performance related to time-domain specification

Controller	Delay time, s	Rise time, s	Peak time, s	Settling time, s	Maximum peak overshoot, %
MFB+ANN	0,05	0,08	0,1	0,6	12
MFB+FLC	0,09	0,15	0,18	0,55	8
MFB+PID	0,15	1,55	1,6	1,65	7

Conclusions. Three different hybrid controllers are designed according to the proposed control approach. The considered speed condition based controller regulated switching signals generated by the artificial neural network/fuzzy logic/proportional integral derivative controllers, which is used to control the output voltage level of bidirectional converter and unidirectional converter related to the motor's speed. Among all the controllers used in this paper, speed condition based controller played a vital role and salted it as a common controller. Three hybrid controllers, speed condition based controller with artificial neural network, speed condition based controller with fuzzy logic, and speed condition based controller with proportional integral derivative are implemented individually to the main circuit in 4-different modes corresponding to the load applied and attain satisfactory results. Performance and comparative analysis are done among the three-hybrid controller by considering distinct time-domain measurements.

Conflict of interest. The authors declare that they have no conflicts of interest.

REFERENCES

1. Chandra Mouli G.R., Bauer P., Zeman M. System design for a solar powered electric vehicle charging station for workplaces. *Applied Energy*, 2016, vol. 168, pp. 434-443. doi: https://doi.org/10.1016/j.apenergy.2016.01.110.

2. Kydd P.H., Anstrom J.R., Heitmann P.D., Komara K.J., Crouse M.E. Vehicle-Solar-Grid Integration: Concept and Construction. *IEEE Power and Energy Technology Systems Journal*, 2016, vol. 3, no. 3, pp. 81-88. doi: https://doi.org/10.1109/JPETS.2016.2558471.

3. Kim N., Biglarbegian M., Parkhideh B. Flexible high efficiency battery-ready PV inverter for rooftop systems. *2018 IEEE Applied Power Electronics Conference and Exposition (APEC)*, 2018, pp. 3244-3249. doi: https://doi.org/10.1109/APEC.2018.8341567.

4. Amin Bambang R.T., Rohman A.S., Dronkers C.J., Ortega R., Sasongko A. Energy Management of Fuel Cell/Battery/Supercapacitor Hybrid Power Sources Using Model Predictive Control. *IEEE Transactions on Industrial Informatics*, 2014, vol. 10, no. 4, pp. 1992-2002. doi: https://doi.org/10.1109/TII.2014.2333873.

5. Katuri R., Gorantla S. Realization of prototype hardware model with a novel control technique used in electric vehicle application. *Electrical Engineering*, 2020, vol. 102, no. 4, pp. 2539-2551. doi: https://doi.org/10.1007/s00202-020-01052-0.

6. Katuri R., Gorantla S. Design and Comparative Analysis of Controllers Implemented to Hybrid Energy Storage System Based Solar-powered Electric Vehicle. *IETE Journal of Research*, 2021, pp. 1-23. doi: https://doi.org/10.1080/03772063.2021.1941328.

7. Akar F., Tavlasoglu Y., Vural B. An Energy Management Strategy for a Concept Battery/Ultracapacitor Electric Vehicle With Improved Battery Life. *IEEE Transactions on Transportation Electrification*, 2017, vol. 3, no. 1, pp. 191-200. doi: https://doi.org/10.1109/TTE.2016.2638640.

8. Kollimalla S.K., Ukil A., Beng G.H., Manandhar U., Tummuru N.R. Optimization of charge/discharge rates of a battery using a two stage rate-limit control. *2017 IEEE Power & Energy Society General Meeting*, 2017, pp. 1-1. doi: https://doi.org/10.1109/PESGM.2017.8273807.

9. Katuri R., Gorantla S. Optimal Performance of Lithium-Ion Battery and Ultra-Capacitor with A Novel Control Technique Used In E-Vehicles. *Journal of New Materials for Electrochemical Systems*, 2020, vol. 23, no. 2, pp. 139-150. doi: https://doi.org/10.14447/jnmes.v23i2.a11.

10. Katuri R., Rao G.S. Modelling and simulation of Math function based controller combined with PID for smooth switching between the battery and ultracapacitor. *Australian Journal of Electrical and Electronics Engineering*, 2019, vol. 16, no. 3, pp. 163-175. doi: https://doi.org/10.1080/1448837X.2019.1640009.

11. Meradji M., Cecati C., Wang G., Xu D. Dynamic modeling and optimal control for hybrid electric vehicle drivetrain. *2016 IEEE International Conference on Industrial Technology (ICIT)*, 2016, pp. 1424-1429. doi: https://doi.org/10.1109/ICIT.2016.7474967.

12. Li X., Ma R., Wang L., Wang S., Hui D. Energy Management Strategy for Hybrid Energy Storage Systems with Echelon-use Power Battery. *2020 IEEE International Conference on Applied Superconductivity and Electromagnetic Devices (ASEMD)*, 2020, pp. 1-2. doi: https://doi.org/10.1109/ASEMD49065.2020.9276135.

13. Zhou H., Zhou Y., Hu J., Yang G., Xie D., Xue Y., Nordstrom L. LSTM-based Energy Management for Electric Vehicle Charging in Commercial-building Prosumers. *Journal of Modern Power Systems and Clean Energy*, 2021, vol. 9, no. 5, pp. 1205-1216. doi: https://doi.org/10.35833/MPCE.2020.000501.

14. Byrne R.H., Nguyen T.A., Copp D.A., Chalamala B.R., Gyuk I. Energy Management and Optimization Methods for Grid Energy Storage Systems. *IEEE Access*, 2018, vol. 6, pp. 13231-13260. doi: https://doi.org/10.1109/ACCESS.2017.2741578.

15. Li X., Wang S. Energy management and operational control methods for grid battery energy storage systems. *CSEE Journal of Power and Energy Systems*, 2021, no. 5, pp. 1026-1040. doi: https://doi.org/10.17775/CSEEJPES.2019.00160.

16. Regad M., Helaimi M., Taleb R., Gabbar H., Othman A. Optimal frequency control in microgrid system using fractional order PID controller using krill herd algorithm. *Electrical Engineering & Electromechanics*, 2020, no. 2, pp. 68-74. doi: https://doi.org/10.20998/2074-272X.2020.2.11.

17. Slama F., Radjeai H., Mouassa S., Chouder A. New algorithm for energy dispatch scheduling of grid-connected solar photovoltaic system with battery storage system. *Electrical Engineering & Electromechanics*, 2021, no. 1, pp. 27-34. doi: https://doi.org/10.20998/2074-272X.2021.1.05.

18. Pakkiraiah B., Sukumar G.D. A new modified MPPT controller for improved performance of an asynchronous motor drive under variable irradiance and variable temperature. *International Journal of Computers and Applications*, 2016, vol. 38, no. 2-3, pp. 61-74. doi: https://doi.org/10.1080/1206212X.2016.1188586.

19. Pakkiraiah B., Durga Sukumar G. Enhanced Performance of an Asynchronous Motor Drive with a New Modified Adaptive Neuro-Fuzzy Inference System-Based MPPT Controller in Interfacing with dSPACE DS-1104. *International Journal of Fuzzy Systems*, 2017, vol. 19, no. 6, pp. 1950-1965. doi: https://doi.org/10.1007/s40815-016-0287-5.

Received 17.09.2022
Accepted 09.12.2022
Published 07.03.2023

R.S. Kumar[1], *Assistant Professor,*
C.S.R. Reddy[2], *Professor,*
B.M. Chandra[3], *Professor,*
[1] Department of Electrical and Electronics Engineering,
Keshav Memorial Institute of Technology, India,
e-mail: rajasathishkumar38@gmail.com (Corresponding Author)
[2] Department of Electrical and Electronics Engineering,
B V Raju Institute of Technology, India,
e-mail: csubbaramireddy2020@gmail.com
[3] Department of Electrical and Electronics Engineering,
QIS College of Engineering and Technology, India,
e-mail: bmoulichandra@gmail.com

How to cite this article:
Kumar R.S., Reddy C.S.R., Chandra B.M. Optimal performance assessment of intelligent controllers used in solar-powered electric vehicle. *Electrical Engineering & Electromechanics*, 2023, no. 2, pp. 20-26. doi: https://doi.org/10.20998/2074-272X.2023.2.04